Citation Information: DOI: 10.1109/TSTE.2020.3042855

Distributed Reactive Power Control Scheme for the Voltage Regulation of Unbalanced LV Grids

Georgios C. Kryonidis, *Member, IEEE,* Kyriaki-Nefeli D. Malamaki, Spyros I. Gkavanoudis, Konstantinos O. Oureilidis, Eleftherios O. Kontis, *Member, IEEE,* Juan Manuel Mauricio, *Senior Member, IEEE,* José María Maza-Ortega, *Member, IEEE,* and Charis S. Demoulias

***Abstract*—This work proposes a new control strategy for the voltage regulation of unbalanced low-voltage (LV) distribution grids with high penetration of distributed renewable energy sources (DRESs). The proposed method uses the available reactive power of DRESs as the primary means for voltage regulation. Furthermore, its distinct feature is the use of a distributed control architecture prioritizing the response of DRESs to maintain the network voltages within permissible limits and minimize the network losses. The prioritization process is locally implemented by each DRES combining two types of information: (a) the sensitivity matrix that quantifies the impact of reactive power variations on the network voltages and (b) voltage measurements along the network. Time-domain and time-series simulations on the IEEE European LV test feeder are performed to evaluate the performance of the proposed method against existing decentralized, distributed and centralized, optimization-based methods.**

***Index Terms*—Distributed renewable energy sources, loss minimization, reactive power control, unbalance, voltage control.**

I. Introduction

A. Background

INCREASING the share of energy from renewable sources is one of the primary objectives set by the European Union (EU) towards the decarbonization of the energy sector. This is also reflected in the EU directive for the promotion of renewable energy sources (RESs), where the target for the RES share in the gross final energy consumption is increased from 20% in 2020 to 32% in 2030 [1]. Consequently, the penetration level of distributed RESs (DRESs) will continue to increase posing a series of technical challenges related to the secure and reliable operation of distribution grids [2].

Considering low-voltage (LV) distribution grids, voltage rise is considered as the most important issue hindering the further increase of DRES penetration [3]. In the literature, various approaches have been proposed to tackle this issue that can be organized into active power control (APC) and reactive power control (RPC) methods. The former includes generation curtailment (GC) [4], demand response (DR) [5], and use of energy storage systems (ESSs) [6], while the latter mainly involves the use of the available reactive power of DRESs [7]. Nevertheless, APC can be regarded as an energy management approach in the long-term, where energy can be curtailed, shifted, stored, etc. This poses several drawbacks which are related to loss of green energy (GC), consumer inconvenience (DR), and additional installation and operation cost (ESSs) [4]–[6]. On the other hand, these shortcomings are effectively addressed using RPC. Thus, RPC is the first solution to be adopted for the voltage regulation, even in LV grids where its effectiveness is reduced due to the high R/X ratio of lines.

This work is part of and supported by the European Union, Horizon 2020 project "EASY-RES" with Grant agreement: 764090.

G. C. Kryonidis, K.-N. D. Malamaki, S. I. Gkavanoudis, K. O. Oureilidis, E. O. Kontis, and C. S. Demoulias are with the School of Electrical and Computer Engineering, Aristotle University of Thessaloniki, Thessaloniki GR 54124, Greece (e-mail: kryonidi@ece.auth.gr; nmalamak@ece.auth.gr; s.gkavan@gmail.com; oureili@yahoo.gr; kontislefteris@gmail.com; chdimoul@auth.gr).

J. M. Mauricio and J. M. Maza-Ortega are with the Department of Electrical Engineering, Universidad de Sevilla, 41092 Sevilla, Spain (e-mail: j.m.mauricio@ieee.org; jmmaza@us.es).

B. Literature Review of RPC Methods

RPC methods can be classified into three main categories based on the adopted control architecture, namely decentralized, centralized, and distributed control schemes [3]. Among them, distributed control schemes have recently started to gain ground for the following reasons: (a) higher robustness to communication failures than centralized solutions [3] and (b) near-optimal network operation compared to the decentralized control schemes [7]. In terms of implementation, distributed control schemes are further divided into two subcategories, i.e., offline and online, that are analytically described below.

In the offline approach, DRESs use distributed algorithms to iteratively solve an optimization problem [7]–[12]. During the solution process, no control actions are performed by the DRESs. After the algorithm is converged, DRESs switch to a new operation point. In [7] and [8], the well-established alternating direction method of multipliers (ADMM) is used to solve a relaxed version of the original optimization problem by adopting the cone relaxation technique. ADMM is also used in [9] in conjunction with a column-and-constraint generation algorithm to minimize network losses. Its distinct feature is the ability of handling network uncertainties. Furthermore, the authors in [10] propose a distributed accelerated dual descent algorithm that outperforms ADMM in terms of convergence time. However, all these methods assume a balanced network, which is unrealistic for LV grids. An improved version of the ADMM is introduced in [11] including the network asymmetries. Additionally, a distributed implementation of the primal-dual gradient algorithm for the optimal operation of unbalanced networks is proposed in [12]. Nevertheless, all the above-mentioned control schemes assume a discrete operation of DRESs. More specifically, each DRES remains idle till the convergence of the algorithm. This fact in conjunction with the large number of iterations for convergence constitutes the application of these methods under fast, time-varying operating conditions highly questionable.

On the other hand, in the online distributed algorithms, the reactive power output of DRESs is updated at each iteration by combining local measurements acquired at the point of interconnection (POI) with the grid and information received by neighbouring DRESs [13]–[19]. In [13], the voltage regulation problem is addressed in three-stages. In the first two stages, each DRES operates autonomously based only on information locally available at the POI with the grid. In case these stages fail, a distributed algorithm is applied to the third stage selecting neighbouring DRESs to contribute to the voltage regulation process. Nevertheless, the selection process is made in an uncoordinated way leading to unnecessary reactive power exchange with the grid and increased network losses. In [14], a dual ascent algorithm is proposed to optimize distribution networks. Nevertheless, the impact of the adopted communication technology on the performance of the proposed method is not investigated. The dual ascent algorithm is also employed in [15] to minimize the reactive power used by the DRESs. However, several approximations are used in the update process of primal variables leading to possible inaccuracies. An online ADMM method is proposed in [16]. The developed method presents fast convergence allowing its implementation in real networks. Nevertheless, this approach leads to steady-state errors, thus increasing the possibility of voltage violations. Furthermore, in [17], the optimization problem is partitioned to several subproblems that are solved using a randomized distributed algorithm, which, however, is characterized by a very small convergence speed. It is worth mentioning that all above-mentioned solutions cannot accurately model existing LV grids, since they consider a balanced operation. Finally, improved online versions of ADMM and dual ascent algorithm that consider the unbalanced behavior of distribution grids are proposed in [18] and [19], respectively. However, the developed methods cannot model the neutral shifting effect, since they assume a perfectly grounding neutral. Moreover, they require an increased number of iterations to converge.

As a common drawback, the above-mentioned methods cannot effectively handle network non-linearities. To overcome this problem, linearized network models are integrated in the proposed distributed algorithms. Consequently, miscalculations may occur under real-field conditions, leading also to possible voltage violations. Furthermore, these methods target at controlling the phase-to-neutral voltages. This is inconsistent with the requirement posed by the IEEE 1547 Standard that RPC should be applied to regulate the positive-sequence voltages [20]. Additionally, according to the literature review, it can be concluded that little research effort has been made to develop online distributed algorithms that minimize network losses, while assuming an unbalanced network operation. Finally, the vast majority of the proposed methods require the continuous monitoring of all the network nodes, putting an increased stress on the communication infrastructure.

C. Main Contributions

In this paper, a new online distributed architecture for the optimal voltage regulation (OVR) of unbalanced LV grids is proposed. Scope of the proposed method is to minimize the network losses by optimally allocating the reactive power among the DRESs. The main contributions are listed below:

- *Introduction of the prioritization concept*: The optimal allocation of the reactive power among the DRESs is implemented by applying priorities to the response of DRESs towards a voltage violation event.
- *Low-complexity*: The prioritization process is locally determined by each DRES combining local measurements and information received via a communication infrastructure.
- *Fast convergence*: Assuming flat start, the proposed method converges to the final operating point in few seconds, thus allowing its implementation under real-field conditions.
- *Limited information exchange*: Contrary to the distributed solutions presented in the literature, the monitoring requirements of the proposed control scheme are limited to network nodes with DRESs.
- *Positive-sequence voltage regulation*: The proposed method regulates the positive-sequence voltages complying with the requirements posed by IEEE 1574 Standard.
- *Validation to full, nonlinear network model*: The performance of the proposed method is assessed using an accurate representation of the LV grid where the neutral conductor is explicitly modelled.
- *Near-optimal solution*: The proposed method presents near-optimal solutions with reduced computational complexity compared to the use of optimization-based techniques.

II. Modeling of LV Distribution Grids

This section presents a preliminary analysis regarding the modeling of LV grids, which is used as an input for the mathematical formulation of the OVR problem presented in Section III. A graphical representation of the topology of a three-phase LV distribution grid with four-wire configuration is presented in Fig. 1, consisting of 3 nodes, namely h, i, and j. Furthermore, a pure resistive behavior is assumed for the grounding impedance, which is the normal case for distribution systems [21]. Considering nodes i and j of Fig. 1, the current flowing through the lines is calculated according to

$$\begin{bmatrix} \bar{I}_{ij}^{a} \\ \bar{I}_{ij}^{b} \\ \bar{I}_{ij}^{c} \\ \bar{I}_{ij}^{n} \end{bmatrix} = \begin{bmatrix} \bar{Y}_{ij}^{aa} & \bar{Y}_{ij}^{ab} & \bar{Y}_{ij}^{ac} & \bar{Y}_{ij}^{an} \\ \bar{Y}_{ij}^{ba} & \bar{Y}_{ij}^{bb} & \bar{Y}_{ij}^{bc} & \bar{Y}_{ij}^{bn} \\ \bar{Y}_{ij}^{ca} & \bar{Y}_{ij}^{cb} & \bar{Y}_{ij}^{cc} & \bar{Y}_{ij}^{cn} \\ \bar{Y}_{ij}^{na} & \bar{Y}_{ij}^{nb} & \bar{Y}_{ij}^{nc} & \bar{Y}_{ij}^{nn} \end{bmatrix} \begin{bmatrix} \bar{V}_{ij}^{a} \\ \bar{V}_{ij}^{b} \\ \bar{V}_{ij}^{c} \\ \bar{V}_{ij}^{n} \end{bmatrix}. \quad (1)$$

Here, $\bar{V}_{ij}^{x}$ stands for the complex voltage drop between nodes i and j, where superscript x indicates either one of the phases a, b, and c or the neutral n. Furthermore, $\bar{I}_{ij}^{x}$ denotes the complex branch current of phase/neutral x flowing between nodes i and j. Finally, $\bar{Y}_{ij}^{xy}$ stands for the self- or the mutual admittance of the four-wire line connecting node i with node j ($(x, y) \in \{a, b, c, n\}$). To improve the readability, (1) is simplified to:

$$\bar{\mathbf{I}}_{ij} = \bar{\mathbf{Y}}_{ij} \bar{\mathbf{V}}_{ij} \quad (2)$$

where $\bar{\mathbf{I}}_{ij}$ and $\bar{\mathbf{V}}_{ij}$ denote the vector of complex currents and voltage drops between nodes i and j, respectively. Furthermore, $\bar{\mathbf{Y}}_{ij}$ is the admittance matrix of the four-wire line that

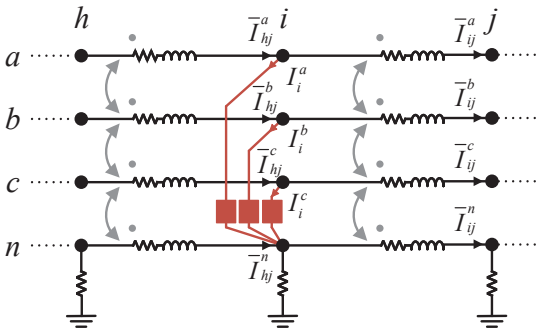

Fig. 1. Simplistic representation of a LV distribution network.

connects node i with node j with a size equal to 4x4. The complex current vector at node i ($\bar{\mathbf{I}}_i$) is can be generally expressed as follows:

$$\bar{\mathbf{I}}_i = \sum_{k\in N\setminus\{i\}} \bar{\mathbf{Y}}_{ki}\bar{\mathbf{V}}_k - \left(\sum_{k\in N\setminus\{i\}} \bar{\mathbf{Y}}_{ki}\right)\bar{\mathbf{V}}_i \tag{3}$$

where N stands for the set of the network nodes. Furthermore, (4) is introduced as additional constraint to satisfy the Kirchhoff's first law at each node.

$$\mathbf{1}^T\bar{\mathbf{I}}_i = \bar{I}_i^g, \quad \forall i \in N \tag{4}$$

Here, $\bar{I}_i^g$ denotes the complex current flowing through the grounding resistance at node i (R_i^g) and can be calculated as follows:

$$\bar{I}_i^g = \frac{\bar{V}_i^n}{R_i^g}, \quad \forall i \in N \tag{5}$$

The apparent power of the network losses can be calculated according to

$$\bar{S}_{\text{loss}} = \sum_{i\in N}\sum_{\substack{j\in N\\ j>i}} \left(\bar{\mathbf{V}}_{ij}^T\bar{\mathbf{I}}_{ij}^*\right). \tag{6}$$

Here, $\bar{\mathbf{V}}_{ij}^T\bar{\mathbf{I}}_{ij}^*$ calculates the apparent power losses of the four-wire line connecting node i with node j.

III. Formulation of the OVR Problem

The voltage regulation with minimum network losses forms an optimization problem. To solve this problem, DRESs are used as controllable reactive power sources. Thus, the optimization problem is transformed into a DRES-based optimal reactive power allocation process which can be mathematically expressed in the following general form:

$$\min f(\mathbf{x},\mathbf{u}) \tag{7a}$$
$$g(\mathbf{x},\mathbf{u}) = 0 \tag{7b}$$
$$h(\mathbf{x},\mathbf{u}) \le 0 \tag{7c}$$

where (7a) stands for the objective function, while (7b) and (7c) are the equality and inequality constraints, respectively. $\mathbf{x}$ denotes the vector of dependent variables , i.e., voltages, as well as branch and node currents of the network. Furthermore, $\mathbf{u}$ is the vector of the control variables, i.e., the reactive power of the DRESs. The mathematical formulation of the OVR problem is analytically presented below.

As mentioned above, the minimization of the network active power losses is the primary optimization objective of the OVR problem and are calculated as follows:

$$f(\mathbf{x},\mathbf{u}) = \Re(\bar{S}_{\text{loss}}) \tag{8}$$

The equality constraints of the optimization problem can be classified into three main categories. The first category involves the equations used to calculate the network losses, the second one includes the power flow equations that model the network operation, while the third one is devoted to the DRES operation.

1) First Category - Network Losses Derivation: The network losses are calculated using (2) and (6).

2) Second Category - Power Flow Equations: The network is modeled using (3)-(5). Furthermore, the relation between net active ($\mathbf{P}_i^{\text{net}}$) and reactive ($\mathbf{Q}_i^{\text{net}}$) power absorbed at each phase of node i and the corresponding node currents and voltages is provided below:

$$\mathbf{P}_i^{\text{net}} = \Re\left(\left(\bar{\mathbf{V}}_i - \bar{V}_i^n\right)^T\bar{\mathbf{I}}_i^*\right), \quad \forall i \in N \tag{9}$$

$$\mathbf{Q}_i^{\text{net}} = \Im\left(\left(\bar{\mathbf{V}}_i - \bar{V}_i^n\right)^T\bar{\mathbf{I}}_i^*\right), \quad \forall i \in N \tag{10}$$

3) Third Category - DRES operation: The net active and reactive power at each node i are calculated according to (11) and (12), respectively.

$$\mathbf{P}_i^{\text{net}} = \mathbf{P}_i^{\text{L}} - \mathbf{P}_i^{\text{D}} \quad \forall i \in N \tag{11}$$

$$\mathbf{Q}_i^{\text{net}} = \mathbf{Q}_i^{\text{L}} - \mathbf{Q}_i^{\text{D}} \quad \forall i \in N \tag{12}$$

Here, $\mathbf{P}_i^{\text{L}}$ and $\mathbf{Q}_i^{\text{L}}$ stand for the active and reactive power absorbed by the load connected to node i, whereas $\mathbf{P}_i^{\text{D}}$ and $\mathbf{Q}_i^{\text{D}}$ are the corresponding active and reactive power of the DRES connected to the same node. It is worth mentioning that $\mathbf{Q}_i^{\text{D}}$ is the only control variable of the OVR problem, while $\mathbf{P}_i^{\text{D}}$ is considered equal to the maximum power the DRES can provide at each time instant.

A distinction is made between the single-phase and three-phase DRESs. It is assumed that the proposed voltage regulation algorithm will be provided by DRESs with three-phase configuration, since it is the dominant type of installation for all kind of DRESs, e.g., PVs. Thus, in the OVR problem, single-phase DRESs are treated as non-controllable active and reactive power sources. Three-phase DRESs are employed as controllable reactive power sources to mitigate voltage violations in the positive-sequence domain as imposed by the IEEE 1547 Standard [20]. The positive-sequence voltage at node i, can be obtained using (13).

$$\bar{V}_i^{pos} = \frac{\bar{V}_i^a}{3} + \frac{\bar{V}_i^b}{3}e^{i\frac{2\pi}{3}} + \frac{\bar{V}_i^c}{3}e^{-i\frac{2\pi}{3}}, \quad \forall i \in N \tag{13}$$

To maintain the network voltages within permissible limits, the following inequality constraints are introduced:

$$V_{\min} \le \left\|\bar{V}_i^{pos}\right\| \le V_{\max}, \quad \forall i \in N \tag{14}$$

where $V_{\min}$ and $V_{\max}$ are the minimum and maximum voltage limits determined by the distribution system operator (DSO). In this paper, the limits posed by the Standard EN 50160 are

considered, i.e., 0.9 and 1.1 p.u., respectively [22]. Finally, (15) represents the boundary limits of the reactive power provided by the DRESs.

$$\mathbf{Q}_{i,\min} \leq \mathbf{Q}_i^{\mathrm{D}} \leq \mathbf{Q}_{i,\max}, \quad \forall i \in N \tag{15}$$

$\mathbf{Q}_{i,\min}$ and $\mathbf{Q}_{i,\max}$ are the minimum and maximum reactive power limits determined by the reactive power capability of the DRES connected at node i [23].

The optimization problem of (2)-(15) is characterized by an increased computational complexity which is mainly caused by three factors. The first corresponds to modelling of network asymmetries, i.e., use of mutual-impedances, neutral point shifting effect, etc. The second is related to the inherent network non-linearities. The third is the extensive size of LV networks. As a result, conventional centralized and distributed optimization methods are rather ineffective, since they suffer from local minimum solutions, initial value problems, and excessive execution times.

IV. Proposed Method

Scope of this section is to present a distributed control scheme for the voltage regulation of unbalanced LV grids. Its distinct feature includes the use of a rule-based approach for the coordination of DRESs presenting reduced computational complexity and monitoring needs compared to the conventional centralized and distributed optimization methods. In the next subsections, the theoretical framework of the proposed method is firstly presented followed by a distributed algorithm for its implementation under real field conditions.

A. Theoretical Framework

As mentioned above, the voltage regulation of LV grids will be mainly carried out by DRESs. In case an overvoltage occurs at a specific network node, the DRES located at this node should absorb reactive power to tackle this problem with the minimum network losses. An analytical proof of this statement is presented in [24]. However, LV grids are characterized by high R/X ratio of the lines. Consequently, when an overvoltage occurs at a specific network node, the available amount of reactive power of the DRES located at the same node will not, most probably, be sufficient for the overvoltage mitigation of this node. As a result, the overvoltage at this node will persist and the reactive power absorption should be undertaken by another DRES of the network.

The selection of the DRES that will contribute to the overvoltage mitigation of this node will be made based on the impact it may have on the network losses. According to the analysis presented in [24], the network losses are increased when the selected DRES is located either downstream or upstream of the node with the overvoltage. Thus, the network losses cannot be used as the main criterion for the selection process. To overcome this issue, the sensitivity of network voltages with respect to reactive power variations is introduced as the main criterion for the selection of the DRES. More specifically, for a given voltage variation at a specific node, a DRES presenting a high sensitivity will need to absorb a smaller amount of reactive power compared to a DRES with a small sensitivity. It is worth mentioning that there is a strong correlation between the overall absorbed reactive power and the network losses. As a result, since the proposed selection method leads to a minimum reactive power absorption, the network losses are also near-minimum.

The theoretical framework of the proposed voltage regulation scheme is summarized in the following example: Let TN is the node of the network with the maximum network voltage. This is regarded as the most crucial node, since the effective mitigation of potential overvoltages at this node indirectly indicates the successful mitigation of overvoltages in the whole LV grid. In case the voltage at TN exceeds $V_{\max}$, the DRES with the highest sensitivity is selected as the regulating DRES (RDRES) to reduce the TN voltage by absorbing reactive power. The RDRES starts absorbing reactive power till one of the following conditions is met:

- *The maximum reactive power of the RDRES is reached*. In such a case, the RDRES selection process is repeated.
- *The maximum network voltage occurs at a different node*. The RDRES selection process is repeated.
- *The overvoltages are finally regulated*. In this case, the voltage regulation process terminates.

Using the above-mentioned concept the network overvoltages are effectively mitigated with near-minimum network losses.

B. Actual Implementation

To pave the way for the implementation of the theoretical framework presented previously under real-field conditions, the distributed control architecture depicted in Fig. 2 is adopted. Following this approach, a two-way communication infrastructure is foreseen to exchange information among the DRESs. More specifically, each DRES is assigned to monitor the positive-sequence voltage of all the DRESs at the POI with the grid ($\mathbf{V}^{\mathrm{pos}}$). Towards this objective, each DRES broadcasts the positive-sequence POI voltage in a regular basis, varying from few milliseconds up to several seconds. It is evident that the refresh rate of the acquired measurements affects the response of the distributed control scheme. The distributed control scheme is implemented by applying to each DRES the control concept of Fig. 3. This control concept describes the dynamic operation of the DRES connected to node j and consists of two operation modes separated by a small deadband (db), where no actions occur in order to prevent oscillations and repeated activation-deactivation cycles. The deadband is determined by the accuracy of the measurement devices located at the DRES, without, however, affecting the performance of the proposed method.

The first operation mode corresponds to the overvoltage mitigation by absorbing reactive power. Assuming that TN is located at node i, this mode is activated in case V_i^{pos} exceeds $V_{\max}$. Nevertheless, to avoid the simultaneous activation of this process in all the DRESs, different time delays are introduced to the response of each DRES ($d_{\mathrm{up},j}$). Scope of the time delays is to prioritize the response of the DRESs in a voltage violation event following the above-mentioned theoretical control concept. After a time delay of $d_{\mathrm{up},j}$, the DRES starts absorbing reactive power by employing a proportional-integral controller to eliminate the error between V_i^{pos} and

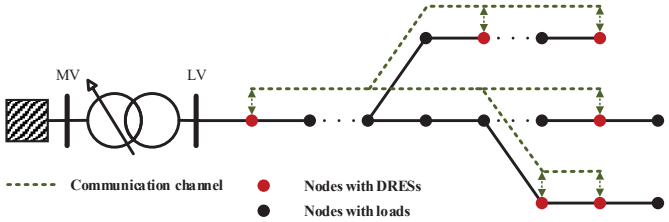

Fig. 2. Distributed architecture of the proposed voltage regulation method.

the target voltage (TV) which is equal to $V_{\max} - 0.5db$. This process continues up to the reactive power capability limit of the DRES unless either the voltage is successfully regulated or the TN is moved to another network node. In the latter case, the process is repeated for the new TN.

The second operation mode includes the reverse process of properly reducing the reactive power consumption. This is activated when V_i^{pos} falls below the voltage threshold ($V_{\max} - db$). After a predefined time delay ($d_{\text{down},j}$), the DRES reduces the reactive power till zero unless either the voltage is regulated or the TN moves to another network node. In the latter case, the process is repeated for the new TN.

C. Time Delays Determination

The time delays are locally determined by each DRES combining two types of information, namely the positive-sequence POI voltages of DRESs and the sensitivity matrix. The former is used to define the TN, while the latter is employed to determine the sensitivity factors that quantify the impact of the reactive power variation of DRESs on the TN voltage. Based on this information, each local controller sorts the sensitivities in a descending order. In this list, the position of each sensitivity determines the time delay of the corresponding DRES. For example, assuming the first operation mode of Fig. 3, if the DRES at node j presents the n-th highest sensitivity, then this DRES will react to any voltage violation event following a time delay of $(n-1)t_d$, where t_d is the time between two successive activations. A similar rationale is used for the determination of the time delays in the second operation mode.

Traditionally, the sensitivity matrix is calculated by inverting the Jacobian matrix used in the Newton-Raphson approach for the power flow analysis of grids [25]. Nevertheless, this solution cannot be adopted in distributed architectures, since all the necessary information, e.g., admittance matrix of the network, power injections at each node, etc., should be gathered in a single unit. To overcome this issue, the method proposed in [26] is adopted for the calculation of the sensitivity matrix. In particular, the sensitivity coefficients are determined using limited, time-invariant information, i.e., line impedances. Thus, it can be readily integrated to the proposed distributed method by calculating offline the sensitivity coefficients and forwarding them to the local controller of DRESs. This process can be undertaken by the DSO and can be repeated in case of network reconfiguration.

Based on the above analysis, the duration of the voltage regulation process (T_{reg}) is equal to Kt_d, where K denotes the number of the activations of the reactive power control scheme among the DRESs. It should be noted that T_{reg} should

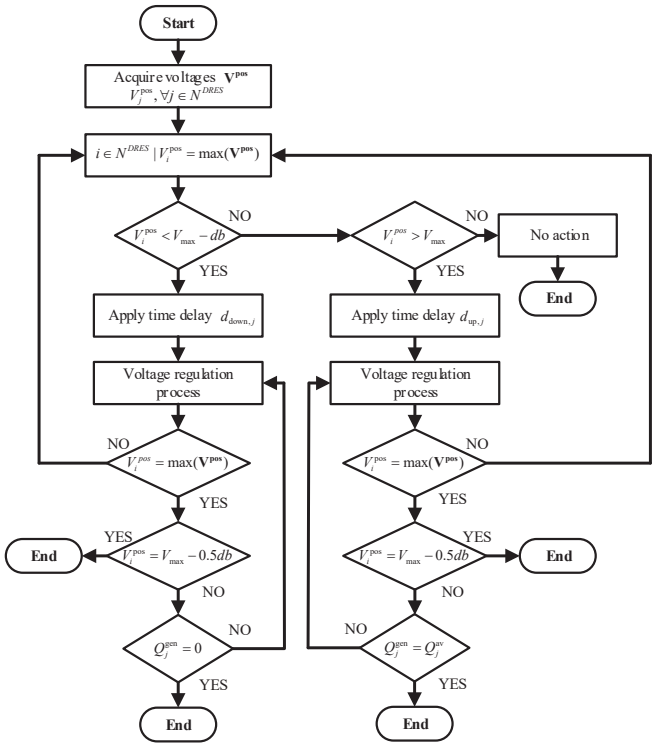

Fig. 3. Reactive power control scheme of the DRES connected to node j.

be less than the activation time of the built-in overvoltage tripping mechanism of DRESs to avoid possible interference. This can be attained by reducing either t_d or K. The former can be implemented using a communication infrastructure that supports fast data exchange with very small latency. The latter can be achieved by grouping the activation of the reactive power control among the DRESs. For example, DRESs with similar sensitivities can be grouped to concurrently react towards a voltage violation event. This way, the number of activations K is reduced, leading to a smaller T_{reg}.

V. Numerical Results

In this section, the performance of the proposed voltage regulation method is assessed by performing time-domain and time-series simulations. The system under study is the 416 V IEEE European LV Test Feeder [27]. The one-line diagram of the examined network is depicted in Fig. 4 and consists of a 906-bus LV network with radial configuration, feeding 55 single-phase loads. To allow the investigation of the proposed voltage regulation of LV grids under real-field conditions, the following modifications are applied to the network of [27]:

- *Introduction of DRESs*. To overcome the absence of DRESs in the original configuration of the IEEE network, 32 three-phase PVs are randomly allocated to the LV network. The connection node and the rated power of the installed PVs is presented in Table I, while the location of each PV is graphically depicted in Fig. 4 using the red square symbol. Note that most of the European DSOs require a three-phase configuration for PVs greater than or equal to 5 kWp. The rated power factor (PF) of PVs is 0.85.
- *Transformation of the line impedance from symmetrical components to the abcn domain to explicitly model the neutral conductor*. The procedure proposed in [28] is adopted.

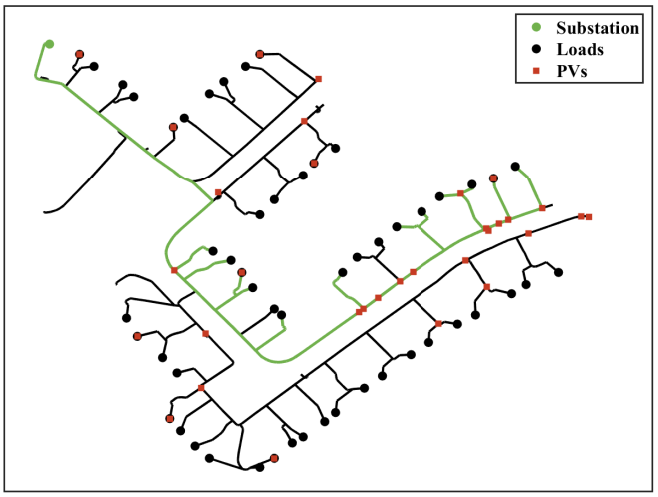

Fig. 4. One-line diagram of the European LV test feeder. The part of grid denoted with green color is used to perform time-domain simulations.

TABLE I
CONNECTION NODE AND RATED POWER OF INSTALLED PVS

Node	kWp	Node	kWp	Node	kWp	Node	kWp	Node	kWp
70	5	320	10	482	5	619	5	861	5
73	10	388	5	556	5	651	5	869	5
166	5	403	5	567	5	681	10	882	10
219	10	447	5	578	10	763	5	884	5
234	5	453	5	580	5	785	5		
247	5	461	10	588	5	794	10		
248	5	476	10	604	10	845	5		

- *Introduction of grounding resistance*. Contrary to the perfectly grounded neutral of the initial configuration, a grounding resistance of 40 Ω is assumed for each neutral node [21].

A. Time-domain Simulations

The performance of the proposed distributed voltage regulation strategy is evaluated by performing time-domain simulations with the PSIM software [29] on a reduced version of the IEEE European LV test feeder depicted in Fig. 4. This modification is made to decrease the execution time of the simulation process to a reasonable value. In particular, the part of the grid denoted with green color is considered in the time-domain simulations, consisting of 250 nodes. Only the PV units and loads directly connected to these nodes are included in these simulations. Their connection node is presented in Table II. Note that loads are numbered according to [27].

The proposed voltage regulation method is evaluated under the worst-case scenario, i.e., maximum generation and minimum consumption, occurring at 13:53 h. At this time instant, the PV units inject their rated power to grid, whereas the absorbed power of the loads is determined by the corresponding profiles described in [27]. Furthermore, to facilitate the network modeling, a balanced network is assumed by considering only the positive sequence components of the lines, whereas loads and PV units with three-phase configuration are considered. Finally, the voltage deadband (db) is considered equal to 0.01 p.u.

TABLE II
CONNECTION NODE OF LOADS AND PVS USED IN THE TIME-DOMAIN SIMULATIONS

PV	247	388	447	453	461	476	482
PV	567	580	588	604	619	651	681
Load	19	20	21	22	29	31	33
Load	34	35	36	37			

Due to page limitation, numerical results related only to the first operation mode are presented. Similar conclusions can be drawn for the second operation mode. The voltage at the slack bus is considered equal to 1.0675 p.u. All the PV units inject their rated power to the LV grid. The maximum network voltage occurs at the POI of PV619 located at node 619. This node is one of the most remotely located nodes with PV units in the network. The RMS value of the voltage magnitude measured by the PV619 is depicted in Fig. 5. It can be observed that the reverse power flow caused by the injected power of the PV units leads to overvoltage.

The reactive power absorption process is activated at 0.4 s. Each PV unit can determine the delay that will be applied towards a voltage violation event by combining the information obtained from the sensitivity theory and the remaining PV units of the network, according to the analysis presented in Section IV-C. The time delays are presented in Table III. For example, PV619 will instantly react to overvoltages, since it presents the highest sensitivity of the voltage at node 619, i.e., the node with the maximum network voltage, with respect to reactive power variations. Moreover, PV588 presents the second highest sensitivity. Thus, the reactive power absorption process will be activated after a time delay of 0.3 s. The time delays of the remaining PV units are presented in Table III. A similar rationale is adopted by the PV units to determine the time delays during the reverse process of properly reducing the reactive power absorption.

To imitate the behavior of the ICT system under real-field conditions, the voltage sent by each PV unit is modeled as a discrete signal with a refreshing period of 50 ms. For example, the voltage sent by PV619 is depicted in Fig. 5 with orange line. It is worth mentioning that relatively small values have been applied to the time delay between two successive activations of the reactive power absorption process as well as to the refresh rate of ICT. This selection has been made to reduce the overall execution time of the time-domain simulation process. Under real-field conditions, these time constants can be increased without, however, affecting the performance of the proposed voltage regulation strategy.

The reactive power output of the PV units participating in the overvoltage mitigation process is presented in Fig. 6, while the maximum network voltage is depicted in Fig. 5.

Initially, PV units operate at unity PF as verified in Fig. 6. At 0.4 s, the proposed voltage regulation control strategy is activated. PV619 instantly reacts to the overvoltage by increasing the reactive power till the minimum PF of 0.85 is reached. According to Fig. 5, the maximum network voltage is reduced but it is still well above the maximum permissible

TABLE III
TIME DELAYS (S) APPLIED TO THE PV UNITS

PV	**247**	**388**	**447**	**453**	**461**	**476**	**482**
d_{up}	3.9	3.3	2.7	3.0	2.4	1.8	2.1
d_{down}	0.0	0.6	1.2	0.9	1.5	2.1	1.8
PV	**567**	**580**	**588**	**604**	**619**	**651**	**681**
d_{up}	1.5	0.6	0.3	3.6	0.0	1.2	0.9
d_{down}	2.4	3.3	3.6	0.3	3.9	2.7	3.0

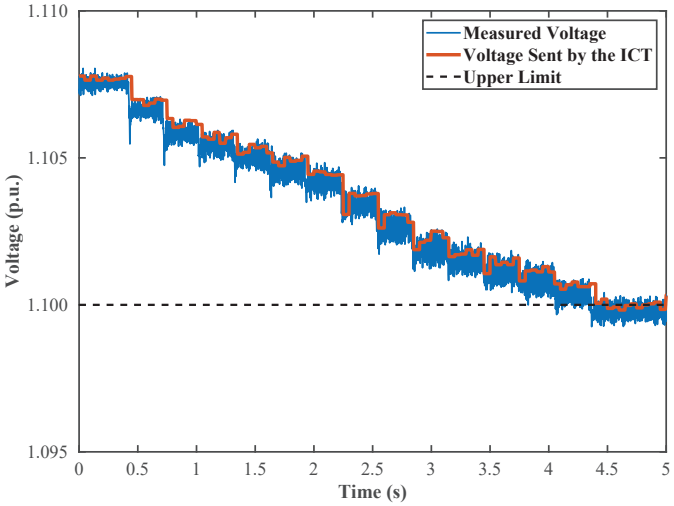

Fig. 5. RMS voltage magnitude at the POI of PV619, where the maximum network voltage occurs.

limit. Thus, after a time delay of 0.3 s, the voltage regulation process continues with the next PV unit in the activation sequence, i.e., PV588, which increases the absorbed reactive power till the minimum PF is reached as shown in Fig. 6. This process continues till the maximum network voltage is finally regulated at 4.4 s. During this process, the activation sequence of the reactive power control among the PV units complies with the time delays presented in Table III. In this way, the reactive power is optimally allocated among the PV units, resulting in near-minimum network losses.

B. Long-term Evaluation

In this subsection, the long-term performance of the proposed voltage regulation method is evaluated by performing time-series simulations using the tool developed in [30]. The simulation period is considered one day with a time resolution of 1 minute. A sunny day is assumed for the PVs using the generation profiles depicted in Fig. 7a. Some indicative consumption profiles of the single-phase loads are presented in Figs. 7b, 7c, and 7d, which are obtained from [27]. It is worth mentioning that the PF of all the single-phase loads remains constant and equal to 0.95 inductive for all the simulation period. The proposed method is compared against decentralized, distributed, and centralized, optimization-based methods. More specifically, the following scenarios are considered:

- High QV (HQV). This is a modified version of the conventional QV (CQV) method. In particular, the settings of $Q(V)$ droop curve, i.e., $V_{\text{th}}^{\text{QV}}$ and $V_{\text{max}}^{\text{QV}}$, are modified from 1.08 p.u. and 1.1 p.u. proposed in [31] to 1.05 p.u. and 1.09 p.u., respectively. The main reason behind this modification is to ensure the overvoltage mitigation by activating of a larger amount of PV units to contribute in the voltage regulation.
- Proposed with target voltage limitation (PWTV). In this scenario, the proposed voltage regulation method is employed with a TV limited to 1.095 p.u.
- Proposed no target voltage limitation (PNTV). To investigate the impact of the selected TV value on the voltage regulation and the network losses, PWTV is modified by considering a TV equal to V_{max}, i.e., 1.1 p.u. This corresponds to the case where db is equal to zero.
- The distributed online VAR control proposed in [19].
- Optimal power flow (OPF). In this scenario, an optimization-based method is considered. Eqs. (2)-(15) are solved at each time instant t using the BARON solver in GAMS [32].

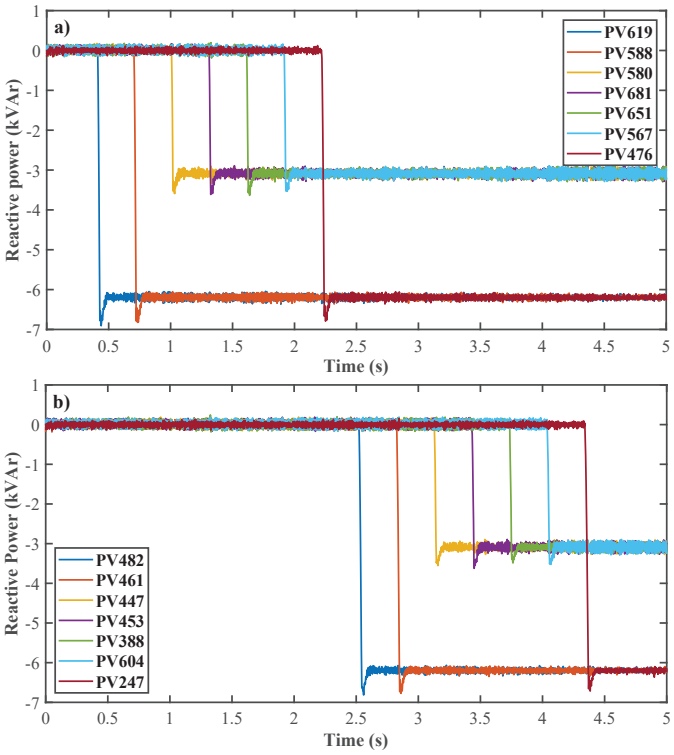

Fig. 6. Reactive power of PVs.

The daily profile of the overall reactive power absorbed by the 32 three-phase PV units is depicted in Fig. 8a, while the daily profile of the maximum network voltage in the positive-sequence domain is presented in Fig. 8b. Moreover, the energy losses of the network are shown in Table IV. Finally, a statistical analysis is performed to investigate the impact of each examined scenario on the voltage asymmetries of the network. The corresponding results are presented in Table V.

According to Fig. 8a, it can be observed that HQV leads to a wider reactive power profile compared to the other examined scenarios. This is justified by the incorporation of the $Q(V)$ droop curve that forces PV units to absorb reactive power in voltages smaller than V_{max}. The impact of this wide reactive power profile on the voltage profile is depicted in Figs. 8b. It is evident that the HQV scenario results in a narrower voltage profile with increased network losses against the other

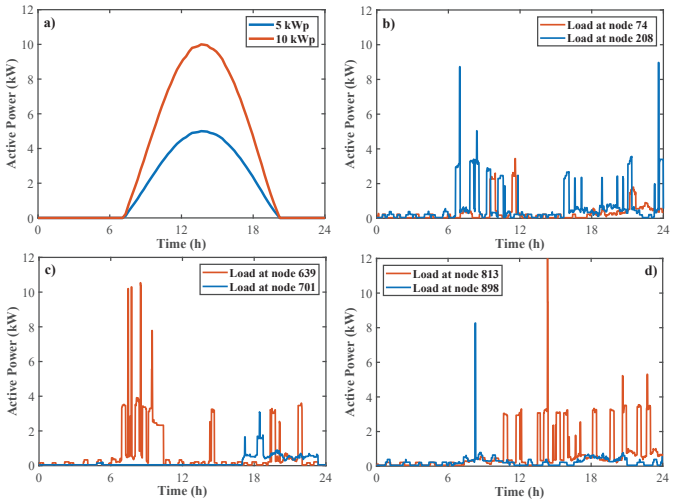

Fig. 7. Daily generation and consumption profiles. a) Generation profiles, b), c), and d) consumption profiles.

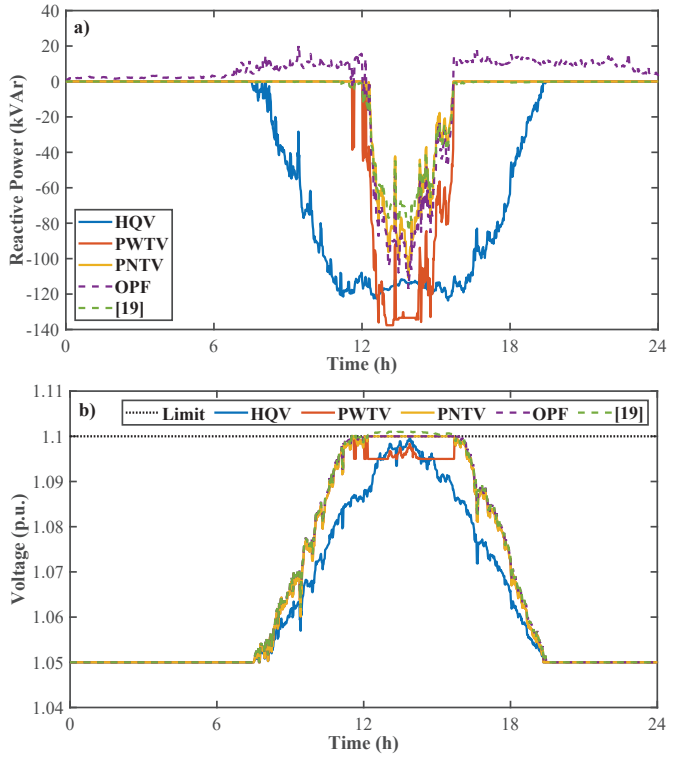

Fig. 8. Daily profiles. a) Overall reactive power consumption and b) maximum network voltage in the positive-sequence domain.

examined implementations. Note that CQV cannot be directly compared with the examined scenarios, since it cannot tackle overvoltages, as shown in Table IV. This is also valid for the distributed algorithm proposed in [19] where it can be observed that overvoltages cannot be effectively tackled, as shown in Fig. 8b. This is justified by the fact that the examined distributed algorithm cannot fully exploit the available reactive power of PVs, as shown in Fig. 8a.

Both implementations of the proposed method, i.e., PWTV and PNTV, outperform HQV, as verified in Figs. 8a, and 8b. More specifically, the daily reactive power profile is improved since the PV units absorb reactive power only when the network voltage exceeds $V_{\max}$, leading also to reduced network losses, as shown in Table IV. Furthermore, according

TABLE IV
DAILY ENERGY LOSSES (KWH)

Examined Scenario	CQV	HQV	PWTV	PNTV	[19]	OPF
Voltage Within Limits	NO	YES	YES	YES	NO	YES
Losses (kWh)	59.42	82.02	63.42	56.21	54.53	55.43
Difference (%)	+7.20	+47.97	+14.41	+1.41	-1.62	0.00

TABLE V
VUF0 (%) AND VUF2 (%) STATISTICAL ANALYSIS OF THE NETWORK NODE WITH THE MAXIMUM VOLTAGE ASYMMETRY

	VUF0				VUF2			
	Mean	**Std**	**Max**	**Min**	**Mean**	**Std**	**Max**	**Min**
HQV	0.68	0.54	4.37	0.03	0.18	0.14	1.12	0.01
PWTV	0.68	0.54	4.30	0.03	0.17	0.14	1.08	0.01
PNTV	0.64	0.51	4.02	0.03	0.17	0.14	1.08	0.01
[19]	0.34	0.36	1.90	0.02	0.26	0.20	1.55	0.01
OPF	0.64	0.51	4.00	0.03	0.17	0.14	1.07	0.01

to Fig. 8b, it can be observed that the introduction of a target voltage TV smaller than $V_{\max}$ increases the overall reactive power absorption, and thus network losses, compared to the case TV is equal to $V_{\max}$. Additionally, there exist time instants where the overall reactive power absorption of PWTV is greater than the HQV. On the other hand, PNTV presents a similar performance to the OPF in terms of the overall reactive power absorption, voltage profile, and network losses.

In terms of network energy losses, PNTV presents a near optimal solution as shown in Table IV. Moreover, the network losses are increased in the PWTV scenario by +14.41% compared to the OPF solution, due to the introduction of the target voltage limitation ($TV = 1.095$ p.u.). Nevertheless, under real field conditions, the target voltage limitation should be also incorporated into the OPF scenario to avoid any voltage violation between two consecutive OPF solutions. In such a case, the corresponding results of the modified OPF scenario and the PWTV will be in a good alignment, as already revealed when comparing PNTV and OPF.

In Table V, VUF0 and VUF2 denote the zero- and the negative-sequence voltage unbalance factors, respectively. It can be observed that the values of VUF2 are well below the limits set by the corresponding standards, i.e., 2% in [20] and 3% in [22]. Considering VUF0, no limits are foreseen by the above-mentioned standards. The decision regarding these limits is mainly left to the discretion of DSOs. However, according to Table V, the mean and the standard deviation of the VUF0 are very small. Thus, it can be concluded that the voltage asymmetries lie within acceptable limits without affecting the secure and reliable operation of the network.

VI. DISCUSSION

In case of LV grids with high R/X ratio, the effectiveness of the RPC is reduced. Thus, it is possible that the available reactive power of DRESs may not be sufficient to regulate the network voltages within permissible limits. To overcome this issue, APC should be employed as a supplementary means for the voltage regulation. It is worth mentioning that RPC

should precede APC in the activation sequence. In this way, the contribution of APC to the voltage regulation is minimized. Further investigations regarding the combined operation of APC and RPC are outside the scope of this paper and constitute future research work.

The proposed voltage regulation method complies with the IEEE 1547 Standard in terms of controlling only the positive-sequence component of the network voltages. Nevertheless, in case of high network unbalances, the zero- and negative-sequence voltages should be also controlled. Although this is not foreseen by the IEEE 1547 Standard, it can be attained by adopting one of the several voltage unbalance mitigation (VUM) techniques proposed in the literature [33]. Furthermore, due to the fact that the proposed voltage regulation method has been implemented in the positive-sequence domain, it can be readily combined with VUM techniques without interfering with each other.

VII. Conclusions

In the paper, a new distributed control scheme is proposed aiming to regulate network voltages of unbalanced LV grids with minimum network losses. According to the proposed method, decisions are locally taken by each DRES combining information from: (a) the sensitivity theory, (b) local measurements, and (c) measurements acquired by the remaining network DRESs. By performing time-domain and time-series simulations, it can be concluded that the proposed method outperforms decentralized solutions and presents a near-optimal behavior compared to optimization-based methods but with reduced computation complexity and monitoring needs.

References

[1] *On the promotion of the use of energy from renewable sources (recast)*, Directive (EU) 2018/2001, Brussels, Belgium, 2018, pp. 1–128.

[2] R. A. Walling, R. Saint, R. C. Dugan, J. Burke, and L. A. Kojovic, "Summary of distributed resources impact on power delivery systems," *IEEE Trans. Power Del.*, vol. 23, no. 3, pp. 1636–1644, July 2008.

[3] K. E. Antoniadou-Plytaria, I. N. Kouveliotis-Lysikatos, P. S. Georgilakis, and N. D. Hatziargyriou, "Distributed and decentralized voltage control of smart distribution networks: Models, methods, and future research," *IEEE Trans. Smart Grid*, vol. 8, no. 6, pp. 2999–3008, Nov. 2017.

[4] R. Tonkoski, L. A. C. Lopes, and T. H. M. El-Fouly, "Coordinated active power curtailment of grid connected PV inverters for overvoltage prevention," *IEEE Trans. Sustain. Energy*, vol. 2, no. 2, pp. 139–147, April 2011.

[5] Q. Xie, H. Hui, Y. Ding, C. Ye, Z. Lin, P. Wang, Y. Song, L. Ji, and R. Chen, "Use of demand response for voltage regulation in power distribution systems with flexible resources," *IET Gener., Transm. Distrib.*, vol. 14, no. 5, pp. 883–892, 2020.

[6] Y. Guo, Q. Wu, H. Gao, X. Chen, J. Østergaard, and H. Xin, "MPC-based coordinated voltage regulation for distribution networks with distributed generation and energy storage system," *IEEE Trans. Sustain. Energy*, vol. 10, no. 4, pp. 1731–1739, 2019.

[7] Y. Wang, T. Zhao, C. Ju, Y. Xu, and P. Wang, "Two-level distributed volt/var control using aggregated PV inverters in distribution networks," *IEEE Trans. Power Del.*, vol. 35, no. 4, pp. 1844–1855, 2020.

[8] C. Feng, Z. Li, M. Shahidehpour, F. Wen, W. Liu, and X. Wang, "Decentralized short-term voltage control in active power distribution systems," *IEEE Trans. Smart Grid*, vol. 9, no. 5, pp. 4566–4576, 2018.

[9] P. Li, C. Zhang, Z. Wu, Y. Xu, M. Hu, and Z. Dong, "Distributed adaptive robust voltage/var control with network partition in active distribution networks," *IEEE Trans. Smart Grid*, vol. 11, no. 3, pp. 2245–2256, 2020.

[10] Z. Tang, D. J. Hill, and T. Liu, "Fast distributed reactive power control for voltage regulation in distribution networks," *IEEE Trans. Power Syst.*, vol. 34, no. 1, pp. 802–805, 2019.

[11] B. A. Robbins and A. D. Domínguez-García, "Optimal reactive power dispatch for voltage regulation in unbalanced distribution systems," *IEEE Trans. Power Syst.*, vol. 31, no. 4, pp. 2903–2913, 2016.

[12] X. Zhou, Z. Liu, C. Zhao, and L. Chen, "Accelerated voltage regulation in multi-phase distribution networks based on hierarchical distributed algorithm," *IEEE Trans. Power Syst.*, vol. 35, no. 3, pp. 2047–2058, 2020.

[13] Y. Wang, M. H. Syed, E. Guillo-Sansano, Y. Xu, and G. M. Burt, "Inverter-based voltage control of distribution networks: A three-level coordinated method and power hardware-in-the-loop validation," *IEEE Trans. Sustain. Energy*, vol. 11, no. 4, pp. 2380–2391, 2020.

[14] S. Bolognani, R. Carli, G. Cavraro, and S. Zampieri, "Distributed reactive power feedback control for voltage regulation and loss minimization," *IEEE Trans. Autom. Control*, vol. 60, no. 4, pp. 966–981, 2015.

[15] Z. Tang, D. J. Hill, and T. Liu, "Distributed coordinated reactive power control for voltage regulation in distribution networks," *IEEE Trans. Smart Grid*, article in press.

[16] Y. Zhang, M. Hong, E. Dall'Anese, S. V. Dhople, and Z. Xu, "Distributed controllers seeking AC optimal power flow solutions using ADMM," *IEEE Trans. Smart Grid*, vol. 9, no. 5, pp. 4525–4537, 2018.

[17] X. Hu, Z. W. Liu, G. Wen, X. Yu, and C. Liu, "Voltage control for distribution networks via coordinated regulation of active and reactive power of DGs," *IEEE Trans. Smart Grid*, vol. 11, no. 5, pp. 4017–4031, 2020.

[18] H. J. Liu, W. Shi, and H. Zhu, "Distributed voltage control in distribution networks: Online and robust implementations," *IEEE Trans. Smart Grid*, vol. 9, no. 6, pp. 6106–6117, 2018.

[19] J. Li, C. Liu, M. E. Khodayar, M. Wang, Z. Xu, B. Zhou, and C. Li, "Distributed online VAR control for unbalanced distribution networks with photovoltaic generation," *IEEE Trans. Smart Grid*, article in press.

[20] "Ieee standard for interconnection and interoperability of distributed energy resources with associated electric power systems interfaces," *IEEE Std 1547-2018 (Revision of IEEE Std 1547-2003)*, pp. 1–138, 2018.

[21] E. S. Thomas, R. A. Barber, J. B. Dagenhart, and A. L. Clapp, "Distribution system grounding fundamentals," in *Rural Elect. Power Conf., 2004*, May 2004, pp. A2–1.

[22] *Voltage Characteristics of Electricity Supplied by Public Distribution Networks*, Standard EN 50160, 2010.

[23] L. Zhang, W. Tang, J. Liang, P. Cong, and Y. Cai, "Coordinated day-ahead reactive power dispatch in distribution network based on real power forecast errors," *IEEE Trans. Power Syst.*, vol. 31, no. 3, pp. 2472–2480, 2016.

[24] G. C. Kryonidis, C. S. Demoulias, and G. K. Papagiannis, "A new voltage control scheme for active medium-voltage (MV) networks," *Elect. Power Syst. Res.*, vol. 169, pp. 53–64, Apr. 2019.

[25] K. Christakou, J. LeBoudec, M. Paolone, and D. Tomozei, "Efficient computation of sensitivity coefficients of node voltages and line currents in unbalanced radial electrical distribution networks," *IEEE Trans. Smart Grid*, vol. 4, no. 2, pp. 741–750, 2013.

[26] M. Brenna, E. De Berardinis, L. Delli Carpini, F. Foiadelli, P. Paulon, P. Petroni, G. Sapienza, G. Scrosati, and D. Zaninelli, "Automatic distributed voltage control algorithm in smart grids applications," *IEEE Trans. on Smart Grid*, vol. 4, no. 2, pp. 877–885, 2013.

[27] IEEE PES. (2016, Feb.) Distribution test feeders. [Online]. Available: http://www.ewh.ieee.org/soc/pes/dsacom/testfeeders/index.html

[28] E. E. Pompodakis, G. C. Kryonidis, C. S. Demoulias, and M. C. Alexiadis, "A generic power flow algorithm for unbalanced islanded hybrid ac/dc microgrids," *IEEE Trans.Power Syst.*, article in press.

[29] PSIM, "Software by powersim technologies," *Professional Version*.

[30] G. C. Kryonidis, E. O. Kontis, A. I. Chrysochos, C. S. Demoulias, D. Bozalakov, B. Meersman, T. L. Vandoorn, and L. Vandevelde, "A simulation tool for extended distribution grids with controlled distributed generation," in *2015 IEEE Eindhoven PowerTech*, June 2015, pp. 1–6.

[31] Comitato Elettrotecnico Italiano, "Regola tecnica di riferimento per la connessione di Utenti attivi e passivi alle reti AT ed MT delle imprese distributrici di energia elettrica," Tech. Rep. CEI 0-16, Sept. 2014.

[32] R. E. Rosenthal, *GAMS: A User's Guide*, GAMS Development Corporation, Washington, DC, USA, 2016.

[33] A. Gastalver-Rubio, E. Romero-Ramos, and J. M. Maza-Ortega, "Improving the performance of low voltage networks by an optimized unbalance operation of three-phase distributed generators," *IEEE Access*, vol. 7, pp. 177 504–177 516, 2019.